Transition Met. Chem. 3, 90–98 (1978)

cept on the $1/k_{obs}$ versus $1/[ox]$ plot for reaction with oxalate ion at the same temperature[8]. It is therefore concluded that the mechanism of the reaction of $[Fe(ppsa)_3]^{4-}$ with oxalate ion is a simple dissociative process. The increase in observed rate constant with oxalate ion concentration to a limiting rate is due to the competition of oxalate ion, and the back reaction process, for the dissociated species rather than attack of oxalate ion on the reactant complex. The mechanism of this reaction is therefore not unique, but in keeping with the behaviour of related iron(II) complexes.

We present further evidence to support our reinterpretation of Dutt and Mottola's kinetic results from reactions of other low-spin iron(II) complexes, with oxalate, citrate (Dutt and Mottola mention the reaction of $[Fe(phen)_3]^{2+}$ with citrate), tartrate, and ethylenediaminetetraacetate. Rate constants for these reactions are compared with those for dissociation (aquation) in the Table; our rate constants are limiting values, *vide supra*, as high concentrations of polycarboxylates have been used. For those reactions which result in complete dissociation of the iron(II) complex, rate constants for reactions with the polycarboxylates are equal, within experimental uncertainty, and considering differences in such experimental conditions as ionic strength, to those for aquation at the same temperatures. For those reactions which go to equilibrium rather than to completion, initial rates are approximately equal to aquation rates. Those reactions which do not go to completion naturally involve the more stable complexes {*eg.* $[Fe(phen)_3]^{2+}$}[9] and/or the less potent carboxylates (*eg.* oxalate), conditions where the incoming ligand competes least effectively. Hexadentate Schiff-base iron(II) complexes, which dissociate extremely slowly[10], react at negligible rates with citrate and oxalate ion. It is interesting that the reaction of $[Fe(bipy)_3]^{2+}$ with citrate does not proceed in reaction mixtures saturated with 2,2′-bipyridyl[11]. All this shows that polycarboxylates act as scavangers rather than nucleophiles in these reactions; a role already established for ethylenediaminetetraacetate[12].

References and Notes

(1) J. Burgess Ed., *Inorganic Reaction Mechanisms, Chem. Soc. Specialist Periodical Report*, London, *1*, 176 (1971); *2*, 168 (1972).

(2) (a) D. W. Margerum, *J. Am. Chem. Soc.*, *79*, 2728 (1957); (b) D. W. Margerum and L. P. Morgenthaler, *J. Am. Chem. Soc.*, *84*, 706 (1962); (c) J. Burgess, *Inorg. Chim. Acta*, *5*, 133 (1971).

(3) (a) J. Burgess, G. E. Ellis, D. J. Evans, A. Porter, R. Wane, and R. D. Wyvill, *J. Chem. Soc. A*, 44 (1971); (b) D. J. Farrington, J. G. Jones, and M. V. Twigg, *J. Chem. Soc. Dalton Trans.*, to be submitted; *Inorg. Chim. Acta*, *25*, L 75 (1977). See also ref. 2b; (c) R. D. Gillard, *Coord. Chem. Rev.*, *16*, 67 (1975).

(4) V. V. S. E. Dutt and H. A. Mottola, *Anal. Chem.*, *49* 319 (1977); this reaction is the basis of an improvement to a novel flow system for the rapid routine determination of iron, *viz.* V. V. S. E. Dutt, A. E. Hanna, and H. A. Mottola, *Anal. Chem.*, *48*, 1207 (1976).

(5) Formation of Fe^{III} oxalate species in the presence of excess oxalate is the driving force for this reaction. Similarly, oxygen is necessary for reaction of $[Fe(phen)_3]^{2+}$ with HO^-. The final product is "ferric hydroxide": G. Nord and T. Pizzino, *Chem. Comm.*, 1633 (1970).

(6) E. R. Gardner, F. M. Mekhail, J. Burgess, and J. M. Rankin, *J. Chem. Soc. Dalton Trans.*, 1340 (1973).

(7) M. V. Twigg, *Inorg. Chim. Acta*, *10*, 17 (1974).

(8) Assuming that $k_2/(k_{-1} + k_2) \approx 0.25$ (*ie.* similar to that for $[Fe(bipy)_3]^{2+}$ (ref 7), values of *ca.* 14×10^{-3} s^{-1} and *ca.* 8×10^{-4} s^{-1} can be estimated for k_1 at 58° and 35° respectively.

(9) Log β_3 = 21.2. for $[Fe(phen)_3]^{2+}$ [H. Irving and D. H. Mellor, *J. Chem. Soc.*, 5222 (1962)], *cf.* log β_3 = 17.8 for $[Fe(5NO_2\ phen)_3]^{2+}$ (C. J. Hawkins, H. Duewell, and W. F. Pickering, *Analyt. Chim. Acta*, *25*, 257 (1961)) and log β_3 = 17.1 for $[Fe(bipy)_3]^{2+}$ [J. H. Baxendale and P. George, *Trans. Faraday Soc.*, *46*, 55 (1950)].

(10) E. R. Gardner, F. M. Mekhail, and J. Burgess, *Internat. J. Chem. Kinetics*, *6*, 133 (1974).

(11) The concentration of 2,2′-bipyridyl would be *ca.* 2×10^{-1} mol ℓ^{-1} in this strong salt solution [H. P. Bennetto and J. W. Letcher, *Chem. Ind.*, 847 (1972); N. P. Komar and G. S. Zaslavskaya, *Russ. J. Phys. Chem.*, *47*, 1642 (1973)]; *cf.* the initial concentration of $[Fe(bipy)_3]^{2+}$, approximately 10^{-4} mol ℓ^{-1} in these experiments.

(12) D. J. Farrington and J. G. Jones, *Inorg. Chim. Acta*, *6*, 575 (1972).

TMC 77/110

Polymeric Coordination Compounds of Nickel(II), Cobalt(II), and Zinc(II) with Oxalate Ions as Symmetric Tetradentate Bridging Ligands

Cornelis G. van Kralingen, Johannes A. C. van Ooijen and Jan Reedijk*

Department of Chemistry, Delft University of Technology, Delft 2208, The Netherlands

(Received July 19th, 1977)

Summary

Coordination compounds having the general formula ML_2Ox are described, with Ox = oxalato dianion; M = Ni, Co and Zn; L = water and imidazoles. The compounds are characterised by chemical analyses, i.r., far-i.r., Raman, ligand field and e.s.r. spectra. Magnetic susceptibility measurements at low temperatures indicate a polymeric structure of anti-ferromagnetically coupled M^{2+} ions.

All physical measurements agree with a polymeric structure built up by oxalate ions as tetradentate bridging ligands forming one-dimensional linear chains. Each metal ion is

* Author to whom all correspondence should be addressed.

coordinated by four oxalate oxygens and two donor atoms (N or O) in distorted octahedron.

For M = Ni, the magnetic susceptibility measurements can be best described with the Heisenberg model including a zero-field splitting; for M = Co, the Ising model gives the best results. The exchange coupling constants, $|J|$, vary from 9–13 cm^{-1}.

Introduction

As part of a research program on the magnetic properties of polynuclear coordination compounds, a system of linear-chain compounds is investigated in which the oxalato anion acts as a tetradentate bridge between two metal ions. Thus far, only two similar chains have been reported, *i.e.* $Fe(H_2O)Ox$[1] and $Cu(NH_3)_2(H_2O)_2Ox$[2]. For the compound $Fe(H_2O)_2Ox$ two independent x-ray determinations have been reported[3, 4]. Each Fe^{II} ion is located at the center of a distorted octahedron whose axial positions are occupied by the oxygen atoms of two water molecules whereas the equatorial positions are occupied by four coplanar oxygen atoms belonging to two different oxalato groups. Barros and Friedberg[5] showed that a rather strong interchain interaction exists in the $Fe(H_2O)_2Ox$ compound. In order to eliminate this interchain interaction, we have prepared and studied a series of compounds having the general formula ML_2Ox, with M = Ni, Co and Zn; L = substituted imidazole; Ox = oxalato dianion.

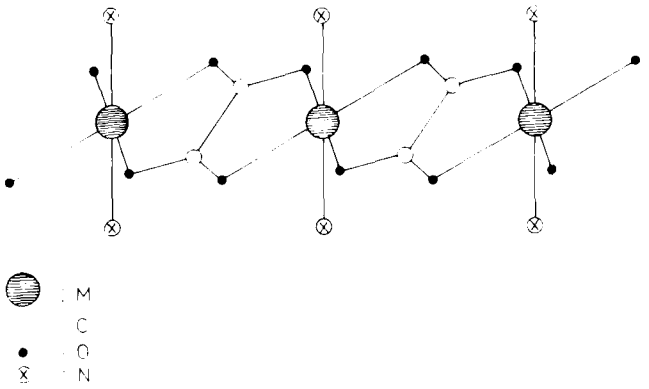

Figure 1. Schematic representation of polymeric ML_2Ox compounds.

In addition, compounds having L = H_2O were investigated for comparison. In Figure 1 the proposed structure of the compounds is illustrated schematically.

Results and Discussion

General

Table 1 lists the compounds with their analytical data. All chemical analyses are in good agreement with the suggested formulae. The nickel compounds are blue, the cobalt compounds are pink, whereas the zinc compounds are white. In addition zinc compounds, doped with 0.1–2.0% Co^{II}, were prepared for e.s.r. measurements (*vide infra*).

X-ray powder diffraction patterns show that compounds with the same ligand but with different metal ions (including Fe^{II}, to be described later) are powder isomorphous, except for water where differences occur in the line positions and relative intensities. Probably the strong interchain hydrogen bridges are responsible for this difference. Another exception is the $Ni(2\text{-}MIz)_2Ox$ compound which has a completely different set of lines, although the i.r. spectra of all 2-MIz compounds are almost identical.

For the $Ni(H_2O)_2Ox$ compound, the water content found by chemical analysis exceeded the theoretical content. This suggests that some additional water molecules are enclosed in the crystal structure. Small differences in the i.r. spectrum of this compound are observed, compared with the other water compounds. Furthermore, some additional differences in the results of the physical measurements occur, *vide infra*.

Table 1. Chemical analysis of ML_2Ox compounds; with Ox = oxalato dianion; M = Ni, Co and Zn; L = water or substituted imidazole

Compound	Found (Calcd.)%			
	C	H	N	M
$Ni(2\text{-}MIz)_2Ox$[a]	38.3 (38.6)	4.1 (3.9)	17.5 (18.0)	18.9 (18.9)
$Co(2\text{-}MIz)_2Ox$	38.0 (38.6)	4.1 (3.9)	17.8 (18.0)	18.7 (19.0)
$Zn(2\text{-}MIz)_2Ox$	37.9 (37.8)	3.9 (3.8)	17.7 (17.6)	20.1 (20.6)
$Ni(DMIz)_2Ox$[b]	42.0 (42.5)	4.8 (4.7)	16.0 (16.5)	17.2 (17.3)
$Co(DMIz)_2Ox$	43.0 (42.5)	4.9 (4.7)	16.5 (16.5)	17.6 (17.4)
$Zn(DMIz)_2Ox$	41.7 (41.7)	4.8 (4.6)	16.0 (16.2)	19.2 (18.9)
$Ni(BIz)_2Ox$[c]	49.2 (50.2)	3.2 (3.1)	14.4 (14.6)	15.3 (15.3)
$Co(BIz)_2Ox$	48.8 (50.1)	3.1 (3.1)	14.2 (14.6)	15.2 (15.4)
$Zn(BIz)_2Ox$	48.4 (49.3)	3.3 (3.1)	14.2 (14.4)	16.7 (16.8)
$Ni(H_2O)_2Ox$	13.1 (13.1)	2.8[d] (2.2)	–	32.0 (32.1)
$Co(H_2O)_2Ox$	13.2 (13.1)	2.5 (2.2)	–	32.3 (32.2)
$Zn(H_2O)_2Ox$	12.9 (12.7)	2.2 (2.1)	–	34.3 (34.5)

a) 2-MIz = 2-methylimidazole.
b) DMIz = 1,2-dimethylimidazole.
c) BIz = benzimidazole.
d) Different samples yielded hydrogen percentages in the 2.8 – 3.0 region (see text).

Infrared and Raman spectra

Infrared spectra were obtained for all compounds and for the free ligands. In addition, Raman spectra of the zinc compounds have been recorded. The spectra show absorptions due to both ligand vibrations and to oxalate vibrations. The i.r. spectra of the compounds with the same ligand are almost identical. Comparison with the i.r. spectra of the free ligands and the Raman spectra of other zinc complexes with

these ligands (ZnL_2Cl_2) yields the position of the oxalate absorptions in the spectra of the new compounds. The wavenumbers of these absorptions for $Zn(2\text{-MIz})_2Ox$ in Table 2 have been listed. Data for Na_2Ox and $Fe(H_2O)_2Ox$ are included because, in these compounds, the oxalate anion is crystallographically known to have D_{2h} symmetry[7]. From the Table it is concluded that, in the new compounds, the oxalate anions also have approximately D_{2h} symmetry and must act as tetradentate ligands. Comparison with the data of complexes, whose crystal structure determinations have proved the tetradentate coordination of the oxalate anions, confirms this[8]. The only difference is that in our compounds the asymmetrical C–O stretching at *ca.* 1650 cm^{-1} is split into two components. This splitting may be due either to a lowering of the lattice site symmetry or a combination band. A similar splitting occurs in some dimeric niobium compounds described by Kergoat and Guerchais[9] in which the oxalate anion also serves as a tetradentate bridging ligand.

Far-i.r. spectra

Far-i.r. spectra were recorded in order to confirm that all our compounds have similar structures and to see if M–L vibrations could be assigned. In the far-i.r. region (500–20 cm^{-1}) the metal oxygen and metal-ligand stretching and bending vibrations occur. The absorptions observed in the 450–50 cm^{-1} region for the ML_2Ox compounds with the ligand bands are listed in Table 3. Also some tentative assignments were made and are included in the Table. It is clear that a strong mixing occurs between the M–Ox, M–L and oxalate vibrations. However, all compounds reveal the same pattern, indicating that the same kind of structure must be present.

Theoretically 8 i.r. active vibrations ($2B_{1u}$, $3B_{2u}$, $3B_{3u}$) for the MO_4N_2 unit under D_{2h} symmetry are expected. However, we have to bear in mind, that by taking such a MO_4N_2 unit to calculate the number of bands one expect, vibrations due to ligand-wagging and ligand-torsion are

Table 2. Oxalate absorptions in the i.r. and Raman spectra

Description			$Zn(2\text{-MIz})_2Ox$		Na_2Ox		$Fe(H_2O)_2Ox$
			Raman	I.r.	Raman	I.r.	I.r.
ν_1	A_g	C–O stretch (sym)	1465		1455		
ν_2	A_g	C–C stretch	915		880		
ν_3	A_g	O–C–O bending (sym)	525		482		
ν_4	A_u	inactive					
ν_5	B_{1g}	C–O stretch (sym)	1630		1642		
ν_6	B_{1g}	C–C–O bending (sym)	585		568		
ν_7	B_{2u}	C–C–O bending (asym)		485		510	480
ν_8	B_{3g}	out of plane	a)		220		
ν_9	B_{2u}	C–O stretch (asym)		1675, 1605[b]	1612	1630	1630[d]
ν_{10}	B_{1u}	out of plane		a)	270[c]		
ν_{11}	B_{3u}	C–O stretch (asym)		1320	1355[c]	1315	1315
$\nu_3 + \nu_{12}$	B_{3u}	combination band		1365		1335	1360
ν_{12}	B_{3u}	O–C–O bending (asym)		800	800[c]	780	815

a) Could not be assigned, because of the strong overlap of this band with the M–Ox and M–L vibrations that occur in the same region.
b) Splitting caused by a small lowering of the lattice site symmetry.
c) Forbidden absorption band.
d) Very broad.

Table 3. Far-i.r. data of the ML_2Ox compounds, with Ox = oxalato dianion; M = Ni, Co and Zn; L = water or substituted imidazole

Compound	Observed absorptions (cm^{-1})											
2-MIz				380m	358m			271s		151m	115m	98m
$Ni(2\text{-MIz})_2Ox$		427m[a]	405m[a]	385s			296s[a]	273m	252m[b]	220w	195m	175m
$Co(2\text{-MIz})_2Ox$		420m[a]	405m[a]	385s			270br[a]			176br		
$Zn(2\text{-MIz})_2Ox$		425m[a]	410w[a]	384s			234br[a]			177m	158s	
DMIz	430m							272s				
$Ni(DMIz)_2Ox$	450s	429m[a]	411m[a]				300s[a]	272m	259m[b]	215m	181m	163m
$Co(DMIz)_2Ox$	443s	413m[a]	396m[a]				273s[a]		239m[b]	196m	162m	147m
$Zn(DMIz)_2Ox$	441s	417m[a]	403m[a]				242s[a]		220w[b]	203m	182m	171w
BIz	416s				270s					241s	227m	155s
$Ni(BIz)_2Ox$	432m	423s[a]	403m[a]		292m	300s[a]			273s[b]	254m	225s	170br
$Co(BIz)_2Ox$	430w	421s[a]	400m[a]		292m	283m[a]			264s[b]	228s	198m	149m
$Zn(BIz)_2Ox$	432m	424m[a]	408m[a]		288m	245s[a]			230s[b]	195w	148s	
$Ni(H_2O)_2Ox$		450vbr[a]			358m[b]		332s[a]		285s[b]	252w	203s	
$Co(H_2O)_2Ox$		445vbr[a]			355m[b]		306s[a]		282m[b]	182s	153m	
$Zn(H_2O)_2Ox$		425vbr[a]			295s[b]		250s[a]		240s[b]	195m	147s	

a) Vibrations with Ox–M–Ox character.
b) Vibrations have M–L character.

74m	106s

neglected. Furthermore, one out-of-plane vibration (B_{1u}) of the oxalato anion occurs at *ca.* 270 cm^{-1}, a region where also M–Ox and M–L stretching vibrations are expected, some of which having the same symmetry and giving rise to coupling of vibrations. The theoretically expected features described here are observed for all compounds by the occurrence of a broad absorption in the 250–300 cm^{-1} region. In addition, absorptions of the free ligand are known to occur in the 200–300 cm^{-1} region. For reasons outlined above, no attempt was made to give a complete far-i.r. data assignment; only Ox–M–Ox and M–L vibrations were assigned.

The sequence of the vibrations Ni–Co–Zn is just as expected from electronegativity and mass of the metal ions; however, the two highest Ox–M–Ox vibrations do not follow this sequence and it is assumed, that these are C–O–M–O–C ring vibrations.

Ligand field spectra

The band maxima, and calculated values of Dq and B for the nickel and cobalt compounds are listed in Table 4. Dq is the ligand field splitting and B the Racah parameter for an octahedral environment of the metal ion. These parameters are calculated using published methods, dealing with averaged environment[10].

The differences in the Dq values may be due to differences in steric hindrance of the various ligands.

Examination of the position of $[Ox]^{2-}$ and H_2O in the spectrochemical series[11] shows that the Dq values in our compounds are unusually high. This may be due to a lattice effect, as is found in some hydrates, or due to a π-back-bonding effect of the symmetrically bridging oxalato anions, resulting in a lowering of the (partly) filled t_{2g} orbitals. The B-values occur in the region expected for octahedral Co^{II} and Ni^{II} compounds.

Electron spin resonance spectra

The e.s.r. parameters of the Co-doped Zn compounds are collected in Table 5. Commonly, these parameters can be used to obtain information about the structure of and the bonding in the compounds. Our main goal was to confirm the tetragonal geometry and to find out a possible deviation from axial symmetry.

To obtain sufficiently sharp resonance lines, the samples have to be cooled below 20 K in order to increase the spin-lattice relaxation time. In this temperature region, high-spin octahedral Co^{II} compounds behave as having ficticious S = 1/2 spin systems.

Theories about the interpretation of spectral data and the relation with ligand field parameters were published as early as 1951 by Abragam and Pryce[12]. They described theoretical curves of $g_{\parallel}$ and $g_{\perp}$ plotted against each other in the weak and strong field approximations for trigonal symmetry.

According to Abragam and Pryce[12] a relationship exists between structural and spectral parameters. The g values are extremely sensitive to small changes in the geometry around the Co^{II} ion.

In Figure 2, our experimental $g_{\parallel}$ and $g_{\perp}$ are plotted against each other and compared with the theoretical plots given by Abragam and Pryce. Most of the spectra show three g values, characteristic for rhombic geometry; in those cases the value $(g_2 + g_3)/2$ was used to calculate $g_{\perp}$. Our experimental values

Table 4. Ligand field data for the ML_2Ox compounds; with Ox = oxalato dianion; M = Ni and Co; L = water or substituted-imidazole

Compound	$^3T_{1g}(P) \leftarrow$ (cm^{-1})	$^3T_{1g}(F) \leftarrow {}^1E_g \leftarrow$ (cm^{-1})	$^3T_{2g} \leftarrow {}^3A_{2g}$ (cm^{-1})	Dq (cm^{-1})	B (cm^{-1})
$Ni(2\text{-}MIz)_2Ox$	26000	16000, 13700sh	9400	940	878
$Ni(DMIz)_2Ox$	26000	15900, 13700sh	9500	945	871
$Ni(BIz)_2Ox$	25060	15600, 13300sh	9000	900	895
$Ni(H_2O)_2Ox$	25060, 27040[a]	15700, 14000sh	9400	935	922
	$^4T_{1g}(P) \leftarrow$ (cm^{-1})	$^4A_{2g} \leftarrow$ (cm^{-1})	$^4T_{2g} \leftarrow {}^4T_{1g}(F)$ (cm^{-1})		
$Co(2\text{-}MIz)_2Ox$	19300	16500sh	8600	940	785
$Co(DMIz)_2Ox$	19400	16500sh	8600	935	795
$Co(BIz)_2Ox$	18900	16500sh	8300	910	775
$Co(H_2O)_2Ox$	20000	17000sh	8500	930	840

a) This splitting is caused by a lowering of the symmetry, probably due to additional water molecules in the crystal lattice (see text).

Table 5. E.s.r. parameters at X-band frequencies of ML_2Ox compounds, with M = 98% Zn and 2% Co (uncertainties in the g values are 0.01; A values are accurate to *ca.* 2G in the ideal splitting case)

Compound	$g_1 = g_{\parallel}$	g_2	g_3	$g_{\perp} = 0.5\,(g_2 + g_3)$	$A_1 = A_{\parallel}$ (G)	A_2 (G)	A_3 (G)
$M(H_2O)_2Ox$	6.28	3.75	2.62	3.19	86	~ 51	~ 24[a]
$M(2\text{-}MIz)_2Ox$	6.29	3.62	2.52	3.07	70[a]	b)	b)
$M(DMIz)_2Ox$	5.51	3.66	3.66	3.66	71	~ 34	
$M(BIz)_2Ox$	5.68	4.20	2.78	3.49	76[a]	b)	b)

a) The hyperfine structure is not completely resolved; [in the ideal case the absorptions split into 8 lines ($M_{I(Co)} = 7/2$ and one expects $2\,1 + 1 = 8$ splittings)].

b) No hyperfine structure is observed.

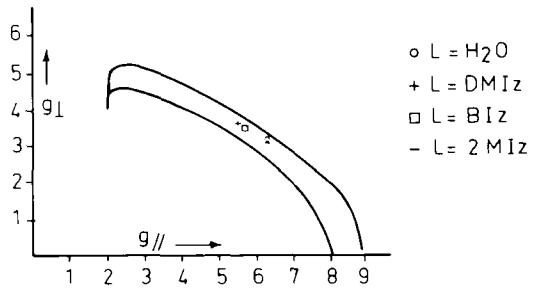

Figure 2. Experimental values of $g_{//}$ plotted against $g_{\perp}$; drawn curves are the theoretical ones for weak-field (upper curve) and strong field (lower curve).

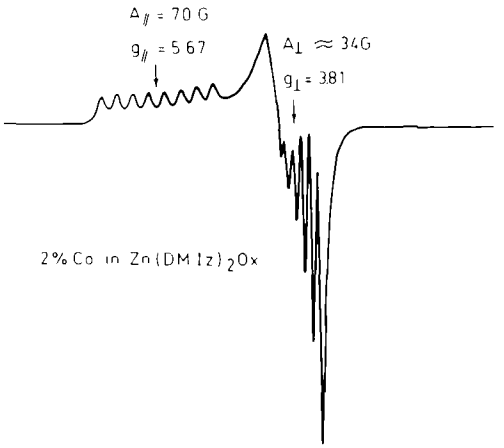

Figure 3. E.s.r. derivative curve of the 2% Co doped $Zn(DMIz)_2Ox$ compound at 4.2 K.

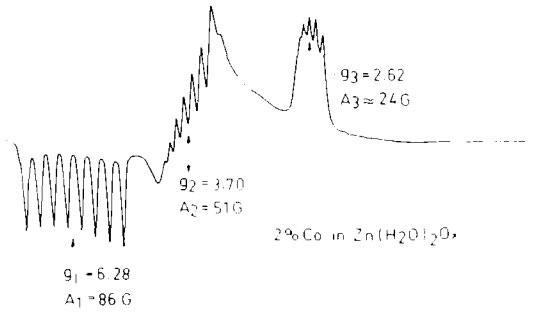

Figure 4. E.s.r. derivative curve of the 2% Co doped $Zn(H_2O)Ox$ compound at 4.2 K.

fall between the two extreme cases of weak-field (upper curve) and strong-field (lower curve). The observed $A_{//}$ values for our compounds are all in the region of 70 G; this value is frequently found for imidazoles that are octahedrally coordinated to Co^{II} and that have $g_{//} > g_{\perp}$ [13].

From the e.s.r. experiment, we can conclude that in the present compounds the Co^{2+} ion is octahedrally coordinated; however, only the DMIz compound shows strict axial symmetry, whereas all others reveal a rhombic distortion. It is remarkable that only for the ligand without an acid N–H group, is axial symmetry observed. This suggests that hydrogen bonding between the azole ligands and the oxalato anions is significant. Two illustrative spectra are drawn in Figures 3 (axial) and Figure 4 (rhombic).

Magnetic measurements

Magnetic susceptibility measurements at low temperature (4.2–100 K) were carried out to determine the sign and magnitude of the exchange coupling between the metal ions and to confirm the linear chain behaviour. For all compounds the susceptibility curves show a broad maximum, indicating that the metal ions are coupled antiferromagnetically. To describe the experimental susceptibility data, a model is needed. The basic properties of the models can be understood from the spin interaction Hamiltonian, *e.g.*[17]:

$$H = -2J \sum_{i,j} (aS_i^z \cdot S_j^z + b(S_i^x \cdot S_j^x + S_i^y \cdot S_j^y)) \qquad (1)$$

where J is the exchange parameter between nearest neighbours, $\sum_{i,j}$ is the summation over all pairs of ions i and j and S^x, S^y and S^z are the components of spin angular moment S. The a/b ratio is an anisotropy parameter.

In many cases, S represents the effective spin operator, utilized in the description of a (2 S + 1)-fold degenerate ground state of a magnetic ion. Crystal field anisotropy may suppress *e.g.* the S^x and S^y components and thereby induce anisotropic exchange.

The a = b = 1 case is called the Heisenberg model in which the magnetic interaction is isotropic. The case of a = 1, b = 0 describes an extreme anisotropic coupling and is called the Ising model. The case a = 0, b = 1 is called the XY model or planar Heisenberg model if it is required that the spins lie within the molecular xy-plane. Determination of the thermodynamic functions starting from the general interaction Hamiltonian (1), gives rise to severe problems. Until now closed form expressions for the partition function could be derived only for the S = 1/2 Ising model[14], the S = 1/2 XY model[15] and for the classical limit $S \to \infty$ with arbitrary spin dimensionality[16]. Numerical approximations concerning the thermodynamic properties of infinite chain systems are available. Bonner and Fisher[17] and Weng[18] applied the methods of extrapolation from limited chain length calculations to obtain thermodynamic values for the infinite chain. Weng neglected the influence of zero-field splitting for ions $S > 1/2$ on the thermodynamics of such chains. In fact all ions with $S > 1/2$ (except those in an S-state) may exhibit a large zero-field splitting. Recently, de Neef[19] published some thermodynamic properties of linear chains with Heisenberg exchange and crystal field anisotropy for S = 1 ions. De Neef found that the influence of the zero-field splitting on the specific heat is more pronounced than on the magnetic suceptibility. Since our data concern only the magnetic susceptibility, in our description of the experimental susceptibility data, both Weng's results and de Neef's results for the S = 1 systems (Ni chains) are considered. For the S = 1/2 systems – as is the case for Co^{2+} at low temperatures – the results of Bonner and Fisher[17] are available, for the Heisenberg model.

Within the Ising model, closed form expressions for the parallel and transverse susceptibility are available for the S = 1/2 systems[20]. For the S = 1 system, Suzuki *et al.*[21] published the parallel susceptibility versus temperature curve. Within the XY model, for S = 1/2 only, the transverse susceptibility has been calculated by Katsura[15]. To the best of our knowledge no theoretical work has been carried out previously for systems $S > 1/2$. In the present paper, the

experimental susceptibility data have been interpreted in the light of the aforementioned calculations and approximations. We are aware of the fact that the listing of possible ways to interpret our magnetic susceptibility data is not complete. Especially in the isotropic case, much more theoretical work has been done, *i.e.* high temperature series expansions[22], Green's function approaches[23], low-temperature approximations[24] (spin wave theory). However, using all these available results would lead us much too far from the goal of this work, namely to find out if we are dealing with chains of high one-dimensionality, and to obtain an indication for the strength of the magnetic interaction.

In the next section, the experimental magnetic susceptibility data of the Ni and Co chains will be described and discussed.

Nickel compounds

All susceptibility versus temperature curves show a broad maximum, typical for antiferromagnetically coupled metal ions. Principally the metal ions can be coupled in three different ways, *i.e.* in dimers, one-dimensional chains and two-dimensional chains. Ginsberg[25] published the theoretical expression for the susceptibility of Ni dimers, but it was not possible to describe our susceptibility data with this expression. Furthermore, Hendrickson, *et al.*[26] has published magnetic data of crystallographically established dimeric oxalato-bridged nickel compounds. Comparing their data with ours it is evident that our susceptibility maxima are much broader and lower, whereas T_{max} is of the same order of magnitude.

Distinguishing between one- and two-dimensional structures from magnetic measurements on powders is more difficult; however, from the i.r. spectra of the compounds under discussion and that of *e.g.* $Fe(H_2O)_2Ox$, it is clear that one-dimensional structures are involved here. Moreover, C–O and C–C–O vibrations differ strongly for the bis-bidentate (one-dimensional) and the tetramonodentate (two-dimensional) cases.

From these arguments, it is assumed that in the present compounds the metal ions are coupled in one-dimensional chains. This is confirmed by the excellent agreement between calculations according to the one-dimensional models and the observed susceptibility data, *vide infra*.

The relevant susceptibility data for the NiL_2Ox compounds are listed in Table 6, together with the J and g parameters obtained for the different one-dimensional models. Within the Heisenberg model, our susceptibility data were fitted to both Weng's and de Neef's results. Weng[18] has published results obtained from extrapolation of limited chain-length calculations, neglecting zero-field splittings. De Neef[19] did the same, but included an axial zero-field splitting D, taking an extra term in the Hamiltonian 1, namely $-D\sum_i(S_i^{z^2} - 2/3)$. Some results according to Weng and de Neef, together with the experimental data of the compound $Ni(2\text{-}MIz)_2Ox$, are plotted in Figure 5. Within the Ising model, the theoretical expression for the parallel susceptibility given by Suzuki, *et. al.*, was used to describe the experimental data[21]:

$$\chi_{/\!/} = \frac{(N \cdot \beta^2 \cdot g^2_{/\!/})}{2kT} \cdot \frac{(1)}{a^2(a+2)} \cdot \left(1 + \frac{4a^3 + 5a^2 - a + 1)}{a[(a+a^{-1})^2 + 8]^{0.5}}\right);$$

with $a = \exp(-2J/kT)$.

However, in no case could a reasonable fit be obtained, probably due to the influence of the perpendicular susceptibility, which is neglected. Because octahedrally coordinated Ni^{II} compounds generally have g-values that are not very anisotropic, it is evident that the powder susceptibility could not be described by taking into account only the $\chi_{/\!/}$ contribution.

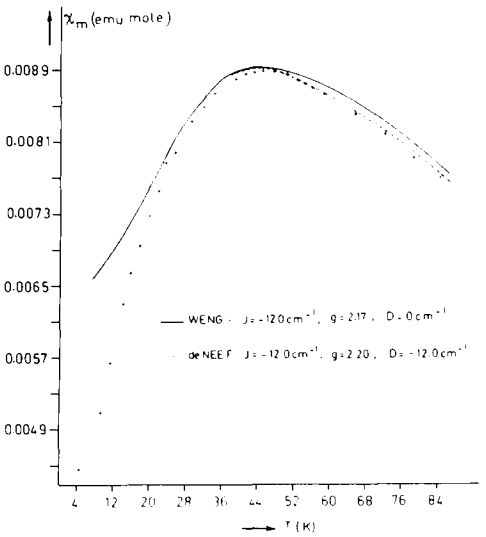

Figure 5. Molar susceptibility χ_m of $Ni(2\text{-}MIz)_2Ox$ as a function of temperature; + = experimental points. The full curve represents the theoretical curve for $J = -12.0\ cm^{-1}$, $D = 0\ cm^{-1}$ and $g = 2.17$ according to the results of Weng. The dotted curve represents the theoretical curve for $J = -12.0\ cm^{-1}$, $D = -12.0\ cm^{-1}$ and $g = 2.20$ according to de Neef's results.

From Figure 5 it is seen that our data can be described very well within the Heisenberg model (for temperatures above *ca.* 40 K), with and without a D-term.

Table 6. Susceptibility data for NiL_2Ox compounds with L = H_2O, 2-MIz, DMIz, BIz. Uncertainties in the last digit are in parentheses

Compound	χ_{max}[a] (emu mole^{-1})	T_{max} (K)	Weng's results $-J(cm^{-1})$	g	de Neef's results (D = −|J|)[b] $-J(cm^{-1})$	g
$Ni(H_2O)_2Ox$	0.00928(9)	41(2)	11.0(4)	2.12(4)	11.5(3)	2.22(2)
$Ni(2\text{-}MIz)_2Ox$	0.00889(9)	45(2)	12.0(2)	2.17(2)	12.0(2)	2.20(1)
$Ni(DMIz)_2Ox$	0.00870(9)	47(2)	12.4(2)	2.18(2)	12.5(2)	2.22(2)
$Ni(BIz)_2Ox$	0.00876(9)	46(2)	12.4(2)	2.19(3)	12.5(2)	2.23(2)

[a] Corrected for diamagnetism of constituent atoms using Pascal's constants[27].
[b] High temperature region.

From these experiments and the knowledge that Ni^{2+} ions, coordinated octahedrally, can exhibit zero-field splittings up to *ca.* 30 cm^{-1} and the fact that even at Q-band frequencies no e.s.r. spectra could be obtained, it is reasonable to assume that describing the susceptibility data within a model including a D-term is the most honest approach. However, the value of this axial zero-field splitting parameter, D, must be regarded only as a rough estimate, because de Neef[18] published results only for values D = nx |J|, with n = −4, −2, −1, 0, +2, +4. The best fits for all our compounds were obtained for the curve with n = −1. The next best fit was obtained by taking the curve with n = 0. (The results of Weng are very close to those of de Neef with N = 0.) The sharp susceptibility decrease at the lowest temperatures can be explained in several ways. A first reason for this decrease could be that the ground state of the Ni^{2+} ion is a nonmagnetic singlet caused by the exchange integral and the D-term. Another explanation is that the Ising system occurs here, but as no expression for the perpendicular susceptibility is known it is not possible to confirm this. However, $g_{\parallel}$ needs to be much larger than $g_{\perp}$ in order to give rise to a large powder-susceptibility decrease at low temperatures and this is seldom found for Ni^{2+} ions. A third explanation could be that anisotropic interchain coupling gives rise to the strong susceptibility decrease. As mentioned above, such an anisotropy is not expected for Ni^{2+} ions.

For the $Ni(H_2O)_2Ox$ compound an increase in susceptibility at very low temperatures was found, indicating the presence of a small amount of paramagnetic impurity. Impurity corrections in the 0.5 to 1.0% range (for different samples) of a monomeric nickel compound was necessary in order to describe the data with Weng's results. This correction hardly effected the susceptibility data in the high temperature region, from which the J/D parameter, n, was calculated.

To find out to what extend the phenomena of zero-field splitting, inter-chain coupling or anisotropic intra-chain coupling are involved, better theories must be awaited. Especially, a description of the low temperature region where these phenomena give rise to serious problems in interpretations, is needed. A first step towards assembly of more experimental data could be the collection of single-crystal susceptibility data; however, so far no crystals have been prepared.

A second reason for the observed increase in susceptibility at lowest temperatures for the $Ni(H_2O)_2Ox$ could be the onset of long-range magnetic order, *i.e.* interchain coupling (*vide infra*). In that case the interchain coupling must be ferromagnetic.

Cobalt compounds

The relevant susceptibility data of the CoL_2Ox compounds, together with the J and g parameters obtained within the Ising model, are given in Table 7. The susceptibility curves again show a broad maximum typical for an antiferromagnetic linear-chain system.

In describing magnetic properties of Co^{2+} ions in an octahedral field, one has to bear in mind that, at very low temperatures, Co^{II} acts as though it had a ficticious spin S = 1/2. In a cubic octahedral field the ^4F orbital state of the free Co^{2+} ion splits into three levels of which the lowest level ^4T, is triply degenerate. Under the action of an axial or rhombic distortion – as is the case in the present compounds (*vide supra*) – of the crystal field in combination with spin-orbit coupling, the ^4T level splits into six Kramers doublets causing the ground state of the Co^{2+} ion to be a doublet. The same energy level remains lowest for all values of the field strength and the splitting between the two lowest lying doublets is so large, that up to *ca.* 20–25 K the system can be described as having a spin S = 1/2. For higher temperatures, thermal occupation of the higher situated Kramers doublets cannot be ignored, resulting in an increase of the susceptibility compared to the fictious S = 1/2 system susceptibility. This would give rise to severe problems in the interpretation of the data. In order to correct for this increase in susceptibility, the energy differences between ground state and the five Kramers doublets must be known and to calculate these energy differences one has to know the crystal field strength and also the spin-orbit coupling constant. Since these parameters are not known for the compounds under discussion, no description of the high temperature part of the susceptibility curves was attempted and so only the low temperature parts were fitted as being S = 1/2 systems in the 4.2–20.0 K region. Within the Heisenberg model, Bonner and Fisher[17] published the extrapolated curve for S = 1/2 ions. Their results, together with Ising and experimental results for $Co(H_2O)_2Ox$, are plotted in Figure 6.

By means of the results[20] for parallel and transverse susceptibility in the Ising model with S = 1/2 and the formula, $\chi_{powder} = 1/3\ \chi_{\parallel} + 2/3\ \chi_{\perp}$, a fit with the experimental sus-

Table 7. Susceptibility data for CoL_2Ox compounds with L = H_2O, 2-MIz, DMIz, BIz. Uncertainties in the last digit are in parentheses

Compound	χ_{Mmax} [f] (emu $mole^{-1}$)	T_{max} (K)	Fitting parameters (Ising model) $g_{\parallel}$ [a]	$g_{\perp}$ [a]	$-J$ (cm^{-1}) [a]	$g_{\perp}$ [b]	$-J$ (cm^{-1}) [b]	C [b,c]	E.s.r. data $g_{\parallel}$	$g_{\perp}$
$Co(H_2O)_2Ox$	0.0425(4)	18.0(5)	6.1(1)	3.3(1)	9.3(3)	3.2(1)	9.1(3)	0.004(5)	6.28(1)	3.19(1)
$Co(2\text{-}MIz)_2Ox$	0.0405(4)	18.5(5)	d)	d)	d)	3.0(1)	9.5(5)	0.049(4)	6.29(1)	3.07(1)
$Co(DMIz)_2Ox$	0.0390(3)	19.5(5)	d)	d)	d)	3.4(2)	10.6(6)	0.042(4)	5.51(1)	3.66(1)
$Co(BIz)_2Ox$	0.0435(4)	15.0(5)	d)	d)	d)	3.3(1)	9.3(4)	0.066(4) [e]	5.68(1)	3.49(1)

a) No impurity correction.
b) Impurity correction included.
c) In units (emu. K. $mole^{-1}$).
d) No fit could be obtained.
e) C-value corresponding to roughly 1% of a monomeric cobalt compound.
f) Corrected for diamagnetism of constituent atoms using Pascal's constants[27].

ceptibility data was tried. The theoretical expressions for parallel and transverse susceptibility are given by:

$$\chi_{\parallel} = \frac{N\beta^2}{4kT} \cdot g^2{}_{\parallel} \cdot \exp(2J/kT)$$

$$\chi_{\perp} = \frac{N\beta^2}{8|J|} \cdot g_{\perp}^2 \cdot \{\tanh(|J|/kt) + (|J|/kT) \cdot [\mathrm{sech}^2(|J|/kT)]\}$$

Within the confines of the XY model, Katsura[15] published the perpendicular susceptibility for an infinite S = 1/2 system.

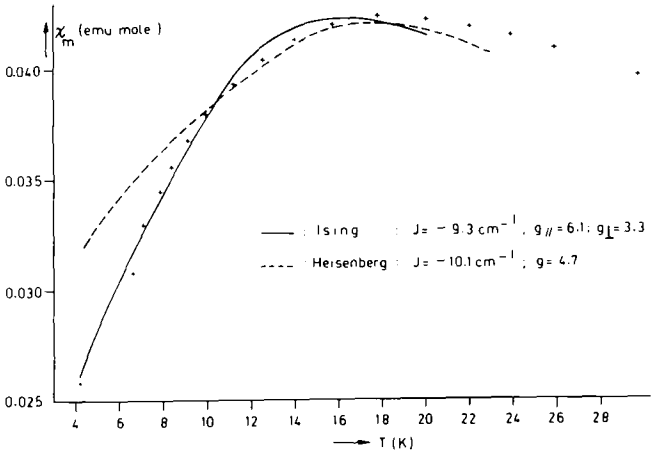

Figure 6. Molar susceptibility χ_m of $Co(H_2O)_2Ox$ as a function of temperature; + = experimental points. The full curve represents the theoretical fit for J = −9.3 cm^{-1}, $g_{\parallel}$ = 6.1 and $g_{\perp}$ = 3.3 according to the Ising model. The dotted curve represents the theoretical fit for J = −10.1 cm^{-1} and g = 4.7 according to the results of Bonner and Fisher.

From Figure 6, it is clear that the Ising model describes the susceptibility data best, especially in the low temperature region where the Heisenberg curve fails. It was not possible to describe the experimental data within the XY model, just as expected, because the influence of the parallel susceptibility on the powder susceptibility is neglected in this model. For all cobalt compounds, a good fit with the experimental data could be obtained neither for the Heisenberg nor for the XY model. This is in agreement with the e.s.r. results, *i.e.* $g_{\parallel} > g_{\perp}$ which is indicative of the presence of an Ising type of interaction. Using a least-squares technique, the data were fitted to the expression for χ_{powder} within the Ising model in two different ways, yielding the values for the parameters listed in Table 7. As mentioned before, the approximation resulting from a fictious S = 1/2 system only holds for temperatures below *ca.* 20 K. In this region small amounts of paramagnetic impurity and inter chain-coupling effects also become important. These effects very strongly influence the $g_{\parallel}$ and to a lesser extent the $g_{\perp}$ and J parameters. For these reasons the data were fitted in two ways:

Firstly, the data were fitted without a correction for a small amount of paramagnetic impurity with parameters $g_{\parallel}$, $g_{\perp}$, and J. Only for the compound with L = H_2O could a reasonable fit be obtained (*viz.* Figure 6). The g parameters, calculated in this way, correlate well with those obtained from the e.s.r data for the compound with L = H_2O.

Secondly, the data were fitted with a correction for the presence of a paramagnetic impurity, having a Curie-like susceptibility C/T. Using fixed $g_{\parallel}$ and $g_{\perp}$, J, and C as parameters the data were fitted within the Ising model. The values for the fixed $g_{\parallel}$ were taken from the e.s.r. data, because these could be obtained with great accuracy for all compounds.Examination of these parameters, listed in Table 7, reveals that for all compounds the $g_{\perp}$ results are in good agreement with the e.s.r. data, indicating that the CoL_2Ox compounds seem to be good examples of one-dimensional Ising compounds. Differently prepared samples of one compound yielded data that could be fitted with slightly different C-values and identical $g_{\perp}$ and J values.

Final remarks

The compounds under discussion appear to be linear-chain coordination compounds, in which the oxalato dianion acts as a tetradentate bridging ligand. The metal ions are antiferromagnetically coupled, with relatively large values for the exchange integral, J. The ligands hardly seem to influence the J-values, in agreement with a super-exchange pathway *via* the O–C–O or O–C–C–O bonds of the oxalato dianion. Qualitatively such a polyatomic bridge having a mirror plane perpendicular to the chain, can be regarded as acting like a molecular orbital and because of the symmetry each metal ion will interact identically with this bridge orbital, giving rise to antiferromagnetic coupling[26].

At present, the corresponding Fe^{II} compounds are being investigated and preliminary Mössbauer experiments reveal that for the compound having L = water at *ca.* 20 K long-range magnetic order, *i.e.* interchain coupling, sets on[28]. However, a second peak in the susceptibility versus temperature curve as published by de Barros and Friedberg[5], could not be detected thus far. This indicates that it is difficult to distinguish between anisotropic intra chain coupling and anti ferromagnetic inter chain coupling from susceptibility measurements alone.

Experimental

Synthesis

All chemicals were commercially available and used without further purification. Ligands used are: water (H_2O), 2-Methylimidazole (2-MIz), 1,2-Dimethylimidazole (DMIz), and Benzimidazole (BIz).

On mixing solutions of the Ni, Co and Zn metal(II) chlorides (5 mmol) and the ligand (20 mmol) in H_2O and of sodium oxalate (5 mmol) in H_2O, very finely divided powders separated. These powders were filtered and washed with dry ethanol and diethyl ether and dried *in vacuo* at room temperature.

Analysis

All samples were checked for purity by chemical analysis (M, C, H, N) and i.r. spectra.

Physical measurements

I.r., far-i.r.-, ligand field-, e.s.r.-spectra, x-ray powder diffraction patterns and magnetic susceptibility measurements, were performed as described elsewhere[6]. Raman spectra of solid samples were obtained using a JEOL Raman spectrometer using Ar and Ne excitation.

Acknowledgement

The authors are indebted to Mr. N. M. van der Pers who recorded the Guinier diagrams. Mr. J. Cornelisse and Mr. C. F. Vermeulen are thanked for doing the C/H/N analyses.

The assistence of Mr. M. J. 't Hart with the far-i.r. spectra is gratefully acknowledged. Dr. M. W. G. de Bolster is kindly thanked for recording the Raman spectra. The authors are indebted to Dr. P. J. van der Put for many valuable discussions. The present investigations have been carried out partly under the auspices of the Netherlands Foundation for Chemical Research (SON) with financial aid from the Netherlands Organization for the Advancement of Pure Research (ZWO).

Note added in press

A recent x-ray structure determination in our department of $Zn(2\text{-}MIz)_2Ox(H_2O)_{0.5}$ has shown that linear chains with tetradentate, symmetric oxalate bridges indeed occur. In this particular case the ligand 2-MIz occur in a *cis* orientation, in agreement with the rhombic e.s.r. spectrum of the Co-doped compound.

References

(1) L. Welo, *Phil. Mag., 6,* 481 (1928).
(2) D. W. Horn and M. A. Graham, *J. Am. Chem. Soc., 39,* 505 (1908).
(3) C. Mazzi and F. Caravelli, *Periodico Mineral. (Rome), 26,* 2 (1957).
(4) S. Cavid, *Bull. Soc. Franc. Mineral. Cristallogr., 82,* 50 (1959).
(5) S. de S. Barros and S. A. Friedberg, *Phys. Rev., 141,* 2 (1966).
(6) J. A. C. van Ooijen and J. Reedijk, *Inorg. Chim. Acta., 25,* 131 (1977).
(7) G. A. Jeffrey and G. S. Parry, *J. Am. Chem. Soc., 76,* 5283 (1954).
(8) N. F. Curtis, *J. Chem. Soc.,* 4109 (1963); N. F. Curtis, *J. Chem. Soc. A,* 1584 (1968); N. F. Curtis, I. R. N. McCormic, T. N. Waters, *J. Chem. Soc. Dalton Trans.,* 1537 (1973); F. Le Floch, J. Sala-Pala, J. E. Guerchais, *Bull. Soc. Chim. France,* 120 (1975); A. C. Skapski, J. E. Guerchais, J. Y. Calves, *C. R. Hebd. Séances Acad. Sci., Sér. C, 278,* 1377 (1974).
(9) R. Kergoat and J. E. Guerchais, *Z. Anorg. Allgem. Chem., 416,* 174 (1975).
(10) J. Reedijk, P. W. N. M. van Leeuwen, W. L. Groeneveld, *Rec. Trav. Chim., 87,* 129 (1968); J. Reedijk, W. L. Driessen, W. L. Groeneveld, *ibid., 88,* 1095 (1969).
(11) C. K. Jorgensen, *Absorption Spectra and Chemical Bonding in Complexes,* Pergamon, London, 1962.
(12) A. Abragam and M. H. L. Pryce, *Proc. Roy, Soc., A 206,* 173 (1951).
(13) J. Reedijk and P. J. J. M. van der Put, *Proc. Int. Conf. Coord. Chem., 16,* 227b (1974).
(14) E. Ising, *Z. Phyzik, 31,* 253 (1925).
(15) S. Katsura, *Phys. Rev., 127,* 1508 (1962).
(16) T. Nakamura, *J. Phys. Soc. Japan, 7,* 264 (1952); M. E. Fisher, *Am. J. Phys., 32,* 343 (1964); H. E. Stanley, *Phys. Rev., 179,* 570 (1969).
(17) J. C. Bonner and M. E. Fisher, *Phys. Rev., A 135,* 640 (1964).
(18) C. Y. Weng, *Ph. D. Thesis,* Carnegie-Mellon Institute of Technology (1968).
(19) T. de Neef, *Ph. D. Thesis,* Eindhoven University of Technology (1975).
(20) M. E. Fisher, *J. Math. Phys., 4,* 124 (1963).
(21) M. Suzuki, B. Tsujiyama, S. Katsura, *J. Math. Phys., 8,* 1 (1967).
(22) G. S. Rushbrooke, G. A. Baker Jr, P. J. Wood, in C. Domb and M. S. Green Eds., *Phase Transitions and Critical Phenomena,* Vol. 3, Academic Press, London.
(23) E. Rhodes and S. Scales, *Phys. Rev., B 8,* 1994 (1973); J. Kondo and K. Yamaji, *Progr. Theor. Physics, 47,* 807 (1972).
(24) T. Keffer in S. Flügge Eds, *Handbuch der Physik,* Vol. XVIII/2. Springer Verlag, Berlin.
(25) A. P. Ginsberg, R. L. Martin, R. W. Brookes, and R. C. Sherwood, *Inorg. Chem., 11,* 2884 (1972).
(26) D. M. Duggan, E. K. Barefield, and D. N. Hendrickson, *Inorg. Chem., 12,* 985 (1973).
(27) E. König, *Magnetic properties of Coordination and Organometallic Transition Metal complexes,* Springer Verlag, Berlin, 1966.
(28) Unpublished observations. TMC 77/71